

**SEGMENTATION OF RETINAL STRUCTURES USING  
IMAGE PROCESSING AND DEEP LEARNING  
TECHNIQUES WITH APPLICATIONS IN RETINAL  
DISEASE PREDICTION**

**ANUMEHA VARMA**



**CENTRE FOR APPLIED RESEARCH IN ELECTRONICS (CARE)  
INDIAN INSTITUTE OF TECHNOLOGY DELHI  
JUNE 2025**

© Indian Institute of Technology Delhi (IITD), New Delhi, 2025

# Segmentation of Retinal Structures Using Image Processing and Deep Learning Techniques with Applications in Retinal Disease Prediction

*by*

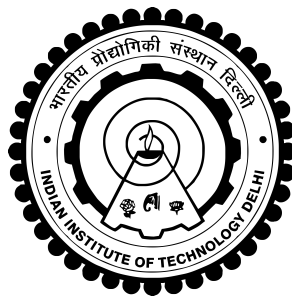
Anumeha Varma

Centre for Applied Research in Electronics (CARE)

*Submitted*

*in partial fulfillment of the requirement of the degree of*

*Doctor of Philosophy to the*



INDIAN INSTITUTE OF TECHNOLOGY DELHI

June 2025

---

*Dedicated to*  
***My Family***

# THESIS CERTIFICATE

This is to certify that the thesis titled **Segmentation of Retinal Structures using Image Processing and Deep learning Techniques with Applications in Retinal Disease Prediction**, submitted by **Anumeha Varma**, to the Indian Institute of Technology, Delhi, for the award of the degree of **Doctor of Philosophy**, is a bona fide record of the research work done by her under our supervision. The contents of this thesis, in full or in parts, have not been submitted to any other Institute or University for the award of any degree or diploma.

**Prof. Monika Aggarwal**  
Professor  
Centre for Applied Research in  
Electronics (CARE)  
IIT-Delhi

Place: New Delhi

Date:

## ACKNOWLEDGEMENTS

First, I'd like to express my deepest gratitude to my supervisor, **Prof. Monika Aggarwal**. She has not only provided invaluable input for my research, but she has also been a constant source of motivation. It has been a privilege to work with someone with immense technical knowledge, attention to detail, and a lot of grace. She has been my true inspiration.

Next, I would also like to convey my sincere thanks to my student research committee members, **Prof. S D Joshi**, **Prof. Prabhu Babu**, and **Prof. Ananjan Basu** for their invaluable comments and suggestions. I am also thankful to the CARE department for providing me with the facilities to conduct my research work.

I am also grateful to my friends, my seniors, and my colleagues at IITD who have been supportive and have helped me either directly or indirectly with my dissertation. I am grateful for the countless joyful memories.

Lastly, I am thankful to my parents, **Mrs. Ranjana Varma** and **Mr. Himanshu Varma**, who have provided me with all the resources and moral support required to continue my education. My brother, **Shalabh Varma**, who consistently helped me overcome any challenges, technical or otherwise, and my sister-in-law, **Prerna Varma**, for her constant support.

# ABSTRACT

**KEYWORDS:** Image decomposition; Retinal fundus image; Vessel segmentation; Deep learning; Illumination correction; Handcrafted Features; Optic Disc; Data Augmentation; Diabetic Retinopathy; Glaucoma; Classification.

Retinal vessels are the only vascular structure that is visible on the outside and can be captured through non-invasive procedures like using a fundus camera. These contain a wide range of information regarding a person's retinal health.

The vessel and optic disc segmentation directly aid in the diagnosis of various diseases, including, but not limited to, DR and glaucoma. The DR features include proliferate symptoms, which are red lesions (microaneurysms and haemorrhages) and bright lesions (soft and hard exudates). The glaucoma features are related to the rim, nerve fiber layer, circumlinear vessel, vessel trunk, optic disc and cup, and laminar dots.

Retinal vessel segmentation has various applications in the biomedical field. This includes early disease detection, biometric authentication using retinal scans, classification, and others. Many of these applications rely critically on an accurate and efficient segmentation technique. In the existing literature, a lot of work has been done to improve the accuracy of the segmentation task, but it relies heavily on the amount of data available for training as well as the quality of the images captured. Another gap is observed in terms of the resources used in these heavily trained algorithms. This work aims to address these gaps by using a resource-efficient unsupervised technique and also increasing the accuracy of retinal vessel segmentation using the Fourier decomposition method (FDM) along with the Gabor transform for image signals. A separate section makes a detailed comparison of the proposed method with several well-known methods and an analysis of the efficiency of the proposed method. The proposed method proves to be efficient in terms of time and resource requirements.

In our second contribution, we focus on thin vessel segmentation. This is an active research problem, with an emphasis on finding a universal approach for different types of fundus datasets. Enhancement of the thin vessels is the first and foremost task for proper segmentation, which is proposed to be done with the total variation (TV) decomposition method with layer-selective enhancement and illumination correction. The vessel segmentation task is carried out on two fronts. For thin vessels, we propose the attention UNet backbone, and for thick vessels, the modified Frangi method is used. The sensitivity perfor-

mance surpasses the state of the art.

Next, once the vessel map is segmented out, we move on to diabetic retinopathy (DR) features. The automated and early detection of symptoms of DR would aid strongly with the diagnosis and cure. In this work, four proliferative symptoms, namely, microaneurysms (MAs), haemorrhages (HAs), hard exudates (HEs), and soft exudates (SEs), are segmented. The red lesions (MAs and HAs) are segmented using mean shift clustering, and the bright lesions (HEs and SEs) are segmented using a basic UNet, concatenated with handcrafted features or feature UNet (FUNet).

This study also presents the use of image processing methods for optic disc segmentation using fine-tuned MedSAM and SegFormer models, which both are transformer-based architectures. Our primary objective is to achieve accurate segmentation of the optic disc in fundus images, which is crucial in diagnosing retinal diseases such as glaucoma and diabetic retinopathy. To refine the segmentation results, we integrated specific pre-processing and post-processing techniques. A comparative study with existing top-tier models reveals that the transformer-based model markedly improves the accuracy of optic disc segmentation.

The automated classification of glaucoma has a major impact on the medical field, and when additional descriptive features of glaucoma are also taken into consideration, it provides further beneficial insights. The images from the JustRAIGS dataset are classified as glaucomatous or not using YOLO V8, and for further classification, the Swin transformer model (STM) is used with data augmentation and ROI limiting.

## सार

रेटिना वाहिकाएं एकमात्र संवहनी संरचना हैं जो बाहर से दिखाई देती हैं और इन्हें फंडस कैमरे का उपयोग करने जैसी गैर-आक्रामक प्रक्रियाओं के माध्यम से पकड़ा जा सकता है। इनमें किसी व्यक्ति के रेटिना स्वास्थ्य के बारे में विस्तृत जानकारी होती है।

वाहिका और ऑप्टिक डिस्क विभाजन विभिन्न रोगों के निदान में सीधे सहायता करते हैं, जिनमें डीआर और ग्लूकोमा शामिल हैं, लेकिन इन्हीं तक सीमित नहीं हैं। डी. आर. विशेषताओं में प्रसार के लक्षण शामिल हैं, जो लाल घाव (माइक्रोएनसिम्स और रक्तस्राव) और चमकीले घाव (नरम और कठोर एक्सुडेट) हैं। ग्लूकोमा की विशेषताएं रिम, तंत्रिका फाइबर परत, परिधीय वाहिका, वाहिका ट्रंक, ऑप्टिक डिस्क और कप और लैमिनार डॉट्स से संबंधित हैं।

रेटिना वाहिका विभाजन के जैव चिकित्सा क्षेत्र में विभिन्न अनुप्रयोग हैं। इसमें जल्दी बीमारी का पता लगाना, रेटिना स्कैन का उपयोग करके बायोमेट्रिक प्रमाणीकरण, वर्गीकरण और अन्य शामिल हैं। इनमें से कई अनुप्रयोग एक सटीक और कुशल विभाजन तकनीक पर गंभीर रूप से निर्भर करते हैं। मौजूदा साहित्य में, विभाजन कार्य की सटीकता में सुधार के लिए बहुत काम किया गया है, लेकिन यह प्रशिक्षण के लिए उपलब्ध डेटा की मात्रा के साथ-साथ कैप्चर की गई छवियों की गुणवत्ता पर बहुत अधिक निर्भर करता है। इन भारी प्रशिक्षित एल्गोरिदम में उपयोग किए जाने वाले संसाधनों के संदर्भ में एक और अंतर देखा जाता है। इस कार्य का उद्देश्य एक संसाधन-कुशल अनसुपरवाइज्ड तकनीक का उपयोग करके इन अंतरालों को दूर करना और छवि संकेतों के लिए गैबर ट्रांसफॉर्म के साथ फूरियर अपघटन विधि (एफडीएम) का उपयोग करके रेटिना वाहिका विभाजन की सटीकता को बढ़ाना है। एक अलग खंड कई प्रसिद्ध विधियों के साथ प्रस्तावित विधि की विस्तृत तुलना करता है और प्रस्तावित विधि की दक्षता का विश्लेषण करता है। प्रस्तावित विधि समय और संसाधन आवश्यकताओं के संदर्भ में कुशल साबित होती है।

हमारे दूसरे योगदान में, हम पतले पात्र विभाजन पर ध्यान केंद्रित करते हैं। यह एक सक्रिय शोध समस्या है, जिसमें विभिन्न प्रकार के फंडस डेटासेट के लिए एक सार्वभौमिक दृष्टिकोण खोजने पर जोर दिया जाता है। उचित विभाजन के लिए पतली वाहिकाओं को बढ़ाना पहला और सबसे महत्वपूर्ण कार्य है, जिसे परत-चयनात्मक वृद्धि और रोशनी सुधार के साथ कुल भिन्नता (टीवी) अपघटन विधि के साथ किया जाना प्रस्तावित है। पोत विभाजन कार्य दो मोर्चों पर किया जाता है। पतली वाहिकाओं के लिए, हम ध्यान यूनेट रीढ़ की हड्डी का प्रस्ताव करते हैं, और मोटी वाहिकाओं के लिए, संशोधित फ्रैंगी विधि का उपयोग किया जाता है। संवेदनशीलता प्रदर्शन कला की स्थिति को पार कर जाता है।

इसके बाद, एक बार वाहिका मानचित्र को विभाजित करने के बाद, हम मधुमेह संबंधी रेटिनोपैथी (डीआर) विशेषताओं की ओर बढ़ते हैं। डी. आर. के लक्षणों का स्वचालित और जल्दी पता लगाने से निदान और इलाज में दृढ़ता से सहायता मिलेगी। इस काम में, चार प्रसारात्मक लक्षण, अर्थात्, माइक्रोएनसिम्स (एमएस) रक्तस्राव (एचएस) हार्ड एक्सुडेट्स (एचईएस) और सॉफ्ट एक्सुडेट्स (एसईएस) को विभाजित किया गया है। लाल घावों (एम. ए. और एच. ए.) को मीन शिफ्ट क्लस्ट्रिंग का उपयोग करके विभाजित किया जाता है, और चमकीले घावों (एच. ई. और एस. ई.) को एक बुनियादी यू. एन. ई. टी. का उपयोग करके विभाजित किया जाता है, जो

हस्तनिर्मित सुविधाओं या सुविधा यू. एन. ई. टी. (एफ. यू. एन. ई. टी.) के साथ जुड़ा होता है।

यह अध्ययन ठीक-ठाक मेडसैम और सेगफोरमर मॉडल का उपयोग करके ऑप्टिक डिस्क विभाजन के लिए छवि प्रसंस्करण विधियों के उपयोग को भी प्रस्तुत करता है, जो दोनों ट्रांसफार्मर-आधारित वास्तुकला हैं। हमारा प्राथमिक उद्देश्य फंडस छवियों में ऑप्टिक डिस्क का सटीक विभाजन प्राप्त करना है, जो ग्लूकोमा और मधुमेह रेटिनोपैथी जैसे रेटिना रोगों के निदान में महत्वपूर्ण है। विभाजन परिणामों को परिष्कृत करने के लिए, हमने विशिष्ट पूर्व-प्रसंस्करण और प्रसंस्करण के बाद की तकनीकों को एकीकृत किया। मौजूदा शीर्ष-स्तरीय मॉडलों के साथ एक तुलनात्मक अध्ययन से पता चलता है कि ट्रांसफार्मर-आधारित मॉडल ऑप्टिक डिस्क विभाजन की सटीकता में उल्लेखनीय रूप से सुधार करता है।

ग्लूकोमा के स्वचालित वर्गीकरण का चिकित्सा क्षेत्र पर एक बड़ा प्रभाव पड़ता है, और जब ग्लूकोमा की अतिरिक्त वर्णनात्मक विशेषताओं को भी ध्यान में रखा जाता है, तो यह आगे लाभकारी अंतर्दृष्टि प्रदान करता है। जस्टरैग्स डेटासेट की छवियों को ग्लोकोमेटस के रूप में वर्गीकृत किया गया है या योलो वी8 का उपयोग नहीं किया गया है, और आगे के वर्गीकरण के लिए, स्विन ट्रांसफॉर्मर मॉडल (एसटीएम) का उपयोग डेटा वृद्धि और आरओआई सीमा के साथ किया जाता है।

# Contents

<b>THESIS CERTIFICATE</b>	<b>i</b>
<b>ACKNOWLEDGEMENTS</b>	<b>ii</b>
<b>ABSTRACT</b>	<b>iii</b>
<b>LIST OF FIGURES</b>	<b>xiii</b>
<b>LIST OF TABLES</b>	<b>xv</b>
<b>ABBREVIATIONS</b>	<b>xvi</b>
<b>1 INTRODUCTION</b>	<b>1</b>
1.1 The Retinal Structure . . . . .	1
1.2 Applications of Segmentation of Retinal Structures . . . . .	2
1.3 Datasets . . . . .	4
1.4 Motivation . . . . .	7
1.5 Contributions . . . . .	8
1.6 Organisation of the Thesis . . . . .	9
<b>2 LITERATURE REVIEW</b>	<b>10</b>
2.1 Preprocessing . . . . .	10
2.2 Retinal Vessel Segmentation . . . . .	10
2.3 Thin Vessel Segmentation . . . . .	12
2.4 Types of Retinal Images . . . . .	13
2.5 Diabetic Retinopathy and Features Segmentation . . . . .	13
2.6 Optic Disc Segmentation and Glaucoma Classification . . . . .	14
2.7 Medical Image Segmentation . . . . .	15
<b>3 IMAGE DECOMPOSITION BASED SEGMENTATION OF RETINAL</b>	

<b>VESSELS</b>	<b>16</b>
3.1 Introduction . . . . .	16
3.1.1 Motivation and Contributions . . . . .	16
3.2 Methodology . . . . .	17
3.2.1 Datasets Used . . . . .	17
3.2.2 Preprocessing Steps . . . . .	18
3.2.3 Segmentation . . . . .	21
3.3 Results and Discussions . . . . .	23
3.3.1 Performance Metrics . . . . .	25
3.3.2 Unsupervised Learning Methods . . . . .	25
3.3.3 Self Supervised Method - Denoising Autoencoders . . . . .	28
3.3.4 Supervised Method - UNet . . . . .	30
3.3.5 Unsupervised Methods for Other Datasets . . . . .	31
3.3.6 Supervised Methods for Other Datasets . . . . .	31
3.3.7 Time and Resource Requirement . . . . .	35
3.3.8 Comparison of Methods . . . . .	35
3.4 Conclusion . . . . .	38
<b>4 THIN VESSEL SEGMENTATION IN FUNDUS IMAGES</b>	<b>39</b>
4.1 Introduction . . . . .	39
4.1.1 Motivation and Contributions . . . . .	39
4.2 Methodology . . . . .	40
4.2.1 Datasets Used . . . . .	40
4.2.2 Preprocessing . . . . .	40
4.2.3 Vessel segmentation . . . . .	42
4.3 Results and Discussions . . . . .	45
4.3.1 Preprocessing . . . . .	45
4.3.2 Thin Vessel Segmentation . . . . .	47
4.3.3 Thick Vessel Segmentation . . . . .	49
4.4 Conclusion . . . . .	54
<b>5 AUTOMATED PROLIFERATE DIABETIC RETINOPATHY FEATURES</b>	

---

<b>SEGMENTATION IN FUNDUS IMAGES</b>	<b>55</b>
5.1 Introduction . . . . .	55
5.1.1 Motivation and Contributions . . . . .	56
5.2 Methodology . . . . .	57
5.2.1 Datasets Used . . . . .	57
5.2.2 Preprocessing . . . . .	58
5.2.3 Red Lesion Segmentation . . . . .	59
5.2.4 Bright Lesion Segmentation . . . . .	60
5.2.5 Postprocessing . . . . .	60
5.3 Results . . . . .	62
5.3.1 Preprocessing . . . . .	62
5.3.2 Microaneurysms . . . . .	62
5.3.3 Exudates . . . . .	67
5.4 Conclusion . . . . .	71
<b>6 OPTIC DISC SEGMENTATION AND GLAUCOMA ABNORMALITY CLASSIFICATION</b>	<b>72</b>
6.1 Introduction . . . . .	72
6.2 Methodology . . . . .	74
6.2.1 Optic Disc Segmentation . . . . .	74
6.2.2 Glaucoma Abnormality Classification using YOLO and SWIN Transformer . . . . .	76
6.3 Results . . . . .	78
6.3.1 Optic Disc Segmentation . . . . .	78
6.3.2 Glaucoma Abnormality Classification using YOLO and SWIN Transformer . . . . .	82
6.4 Conclusion . . . . .	83
<b>7 OVERALL CONCLUSION AND FUTURE SCOPE</b>	<b>84</b>
7.1 Conclusion . . . . .	84
7.2 Future Work . . . . .	85
<b>BIBLIOGRAPHY</b>	<b>86</b>

---

<b>LIST OF PAPERS BASED ON THESIS</b>	<b>104</b>
<b>TECHNICAL BIOGRAPHY OF THE AUTHOR</b>	<b>105</b>

## List of Figures

1.1	The retinal structure. The image is taken from <a href="https://www.virginiaeyeconsultants.com/procedures/eye-conditions/retina/">https://www.virginiaeyeconsultants.com/procedures/eye-conditions/retina/</a> . . . . .	1
1.2	Forus fundus camera. The image is taken from <a href="https://www.forushealth.com/3nethra-classic.html">https://www.forushealth.com/3nethra-classic.html</a> . . . . .	2
1.3	IDRiD_61 image and the lesion ground truths. MAs, HAs, hard and soft exudates. . . . .	3
1.4	Lesions without any other structure around, and lesions near vessel. . . . .	3
1.5	Retinal structures for segmentation . . . . .	5
3.1	Preprocessing steps on a DRIVE dataset image . . . . .	20
3.2	Steps for applying FDM . . . . .	24
3.3	Overall scheme for segmentation . . . . .	24
3.4	a) FDM segmented DRIVE 19 image. b) Gabor with scaling 4 segmented Drive 19 image. c) FDM + Gabor scaling 4 segmented DRIVE 19 image. d) Ground truth DRIVE 19 image. e) Overlapping image of c and d (Red is the ground truth and green is our result). . . . .	28
3.5	a) Post processed, FDM denoised, and autoencoder segmented DRIVE 1 image. b) Ground truth Drive 1 image. . . . .	29
3.6	a) Post processed CDF9/7 UNet DRIVE 1 image. b) Ground truth Drive 1 image. . . . .	31
3.7	a) Proposed unsupervised method based segmentation on Stare 0163 image. b) Ground truth Stare 0163 image. . . . .	32
3.8	a) Proposed unsupervised method based segmentation on HRF 07_g image. b) Ground truth HRF 07_g image. . . . .	32
3.9	a) FDM method based segmentation on Chase 11R image. b) Ground truth Chase 11R image. . . . .	32
3.10	a) Supervised method based segmentation on HRF 15_h image. b) Ground truth HRF 5_h image. . . . .	33
3.11	a) Supervised method based segmentation on STARE im0081 image. b) Ground truth STARE im0081 image. . . . .	33
3.12	An overall comparison on the accuracy of different segmentation techniques on the DRIVE dataset. . . . .	36

3.13	An overall comparison on the sensitivity of different segmentation techniques on the DRIVE dataset. . . . .	36
3.14	An overall comparison on the specificity of different segmentation techniques on the DRIVE dataset. . . . .	38
4.1	The overall segmentation scheme. . . . .	44
4.2	The noise, base and detail layers, respectively, of image 'Image_03L' from CHASE_DB1 dataset. . . . .	45
4.3	Base illumination correction . . . . .	46
4.4	A patch selected from the chase image 'Image_03L' to show the affect of varying $\alpha$ values. . . . .	47
4.5	The original, half to maximum entropy, maximum entropy enhanced images from datasets CHASE_DB1, DRIVE and HRF. . . . .	48
4.6	The unprocessed output sample from the attention UNet for HRF, CHASE_DB1 and DRIVE test sets. . . . .	48
4.7	Zoomed vessel segments showing broken thick vessels from figure 4.6 . . .	49
4.8	The final segmentation result of HRF dataset. . . . .	51
4.9	The final segmentation result of CHASE_DB1 dataset. . . . .	52
4.10	The final segmentation result of DRIVE dataset. . . . .	53
4.11	The final segmentation result of STARE dataset. . . . .	53
5.1	DR effects labelled on the image 73 from the testing set IDRiD dataset [PPK <sup>+</sup> 18]. . . . .	56
5.2	Overall scheme. . . . .	62
5.3	Detail enhanced and base corrected input image. . . . .	63
5.4	Further preprocessing steps: thresholded image, CLAHE enhanced image and blurred image . . . . .	63
5.5	MSC output, and vessel mask generation . . . . .	64
5.6	TPs and FPs with changing patch sizes . . . . .	65
5.7	TPs and FPs with changing radius . . . . .	65
5.8	TPs and FPs with changing radius . . . . .	65
5.9	Final MAs detected for IDRiD . . . . .	66
5.10	Final MAs detected for Eophtha . . . . .	67
5.11	The final predicted HEs for IDRiD . . . . .	69
5.12	Final HEs detected for Eophtha . . . . .	69

5.13	The final predicted HAs for IDRiD . . . . .	70
5.14	The final predicted SEs for IDRiD . . . . .	70
6.1	<i>Schematic representation of finetuning transformers . . . . .</i>	73
6.2	<i>a. Fundus image titled 'drishtiGS_008' taken from DRISHTI-GS1 dataset. b. Optic disc ground truth. . . . .</i>	74
6.3	Flow Diagram of Method1 . . . . .	77
6.4	Flow Diagram of Method2 . . . . .	78
6.5	<i>RGB Channels . . . . .</i>	78
6.6	<i>RGB Channels After CLAHE . . . . .</i>	79
6.7	<i>LAB Channels . . . . .</i>	79
6.8	<i>LAB Channels After CLAHE . . . . .</i>	79
6.9	<i>OD Segmentation Results using MedSAM on DRISHTI-GS1 Dataset . . .</i>	80
6.10	<i>OD Segmentation Results using MedSAM on DRISHTI-GS1 Dataset(IoU Loss) . . . . .</i>	80
6.11	<i>OD Segmentation Results using MedSAM(LAB channels) on DRISHTI-GS1 Dataset . . . . .</i>	80
6.12	<i>OD Segmentation Results using SegFormer on DRISHTI-GS1 Dataset . . .</i>	81
6.13	<i>Postprocessing . . . . .</i>	81

## List of Tables

1.1	Comparison of some popular biometrics [FNM19],[MP20],[Li09] . . . . .	4
1.2	Summary of retinal datasets . . . . .	5
3.1	Wavelet Transform on preprocessed DRIVE dataset. . . . .	26
3.2	Image decomposition methods on preprocessed DRIVE dataset. . . . .	27
3.3	Post processing on unsupervised learning results. . . . .	28
3.4	Segmentation using denoising autoencoders on the DRIVE dataset. . . . .	29
3.5	Post processed autoencoder segmentation results. . . . .	29
3.6	UNet segmentation on the DRIVE dataset. . . . .	30
3.7	Post processed UNet segmentation results. . . . .	30
3.8	Image decomposition methods on other datasets. . . . .	31
3.9	K-Fold cross validation on the stare dataset with CDF 9/7 processing and UNet segmentation. . . . .	34
3.10	Supervised method based segmentation on other datasets. . . . .	34
3.11	Approximate time and resource requirements on 20 images of DRIVE dataset. . . . .	35
3.12	Comparison with the state-of-the-art segmentation methods. . . . .	37
4.1	Contrast difference for varying alpha values . . . . .	46
4.2	Shannon’s entropy values for varying alpha values . . . . .	47
4.3	Scale range for various datasets . . . . .	49
4.4	Scale range effect for HRF dataset image . . . . .	50
4.5	Frangi parameters for HRF dataset image . . . . .	50
4.6	Frangi parameters for CHASE_DB1 dataset image . . . . .	50
4.7	Frangi parameters for DRIVE dataset image . . . . .	51
4.8	Comparison with the state of the art . . . . .	52
4.9	Comparison of cross experimentation on STARE with the state of the art . . . . .	54
5.1	TPs and FPs with changing patch size and radius . . . . .	66

---

5.2	Comparison with the state of the art . . . . .	66
5.3	The parameters for MSC on HEs . . . . .	67
5.4	The segmented exudates and HAs . . . . .	68
6.1	Training parameters for Method 1 . . . . .	77
6.2	Training details for Method 2 using YOLO-based ROI extraction . . . . .	78
6.3	Performance on DRISHTI-GS1 dataset for different loss functions and models	81
6.4	State of the art comparison over accuracy . . . . .	82
6.5	Results of the algorithms in Development phase . . . . .	82

# ABBREVIATIONS

<b>AFF</b>	Adaptive Feature Fusion
<b>AHE</b>	Adaptive Histogram Equalization
<b>AMD</b>	Age-Related Macular Degeneration
<b>ANRI</b>	Appearance Neuroretinal Rim Inferiorly
<b>ANRS</b>	Appearance Neuroretinal Rim Superiorly
<b>AVR</b>	Artery to Vein Ratio
<b>BCLVI</b>	Baring Circumlinear Vessel Inferiorly
<b>BCLVS</b>	Baring Circumlinear Vessel Superiorly
<b>BL</b>	Bright Lesion
<b>CV</b>	Cross Validation
<b>CDF</b>	Cohen–Daubechies–Feauveau
<b>CDR</b>	Cup-to-Disc Ratio
<b>CHASE</b>	Child Heart and Health Study in England
<b>CLAHE</b>	Contrast Limited Adaptive Histogram Equalization
<b>CNN</b>	Convolutional Neural Network
<b>CRAUNet</b>	Cascaded Residual Attention U-Net
<b>DH</b>	Disc Hemorrhages
<b>DoS</b>	Degree of Smoothing
<b>DR</b>	Diabetic Retinopathy
<b>DRIVE</b>	Digital Retinal Images for Vessel Extraction
<b>DWT</b>	Discrete Wavelet Transform
<b>ECG</b>	Electrocardiogram
<b>EEG</b>	Electroencephalography
<b>EMD</b>	Empirical Mode Decomposition
<b>FA</b>	Fluorescein Angiography
<b>FDM</b>	Fourier Decomposition Method
<b>FFT</b>	Fast Fourier Transform
<b>FIBF</b>	Fourier Intrinsic Band Functions
<b>FN</b>	False Negative
<b>FoV</b>	Field of View
<b>FP</b>	False Positive
<b>FP</b>	Fundus Photography
<b>FT</b>	Fourier Transform
<b>FUNet</b>	Feature UNet

---

<b>GE</b>	Green Channel Extraction
<b>GWO</b>	Grey Wolf Optimisation
<b>HA</b>	Haemorrhage
<b>HE</b>	Hard Exudate
<b>HH</b>	High-High
<b>HL</b>	High-Low
<b>HRF</b>	High-Resolution Fundus
<b>IDMWT</b>	Inverse Discrete Multiwavelet Transform
<b>IDRiD</b>	Indian Diabetic Retinopathy Image Dataset
<b>IMF</b>	Intrinsic Mode Function
<b>JPEG</b>	Joint Photographic Experts Group
<b>LC</b>	Large Cup
<b>LD</b>	Laminar Dots
<b>LH</b>	Low-High
<b>LL</b>	Low-Low
<b>LoG</b>	Laplacian of Gaussian
<b>LOO-CV</b>	Leave One Out Cross Validation
<b>LPF</b>	Low Pass Filter
<b>MA</b>	Microaneurysm
<b>MFCA</b>	Multi-Scale Fusion Channel Attention
<b>MSC</b>	Mean Shift Clustering
<b>MSS</b>	Multi-Level Semantic Supervision
<b>NLM</b>	Non-Local Mean
<b>NPDR</b>	Non-Proliferative Diabetic Retinopathy
<b>NRG</b>	No Referable Glaucoma
<b>NVT</b>	Nasalisation of Vessel Trunk
<b>OCTA</b>	Optical Coherence Tomography Angiography
<b>OC</b>	Optic Cup
<b>OD</b>	Optic Disc
<b>PDR</b>	Proliferative Diabetic Retinopathy
<b>PPM</b>	Portable Pixmap
<b>RCNN</b>	Region-based Convolutional Neural Network
<b>RG</b>	Referable Glaucoma
<b>RGB</b>	Red, Green, Blue
<b>RGC</b>	Retinal Ganglion Cell
<b>RNFLDI</b>	Retinal Nerve Fiber Layer Defect Inferiorly
<b>RNFLDS</b>	Retinal Nerve Fiber Layer Defect Superiorly
<b>sEMG</b>	Surface Electromyogram
<b>SE</b>	Soft Exudate
<b>SGD</b>	Stochastic Gradient Descent

---

<b>SNR</b>	Signal to Noise Ratio
<b>SFA</b>	Scale-Aware Feature Aggregation
<b>SLO</b>	Scanning Laser Ophthalmoscope
<b>STARE</b>	Structured Analysis of the Retina
<b>SVSN</b>	Shallow Vessel Segmentation Network
<b>TN</b>	True Negative
<b>TP</b>	True Positive
<b>TV</b>	Total Variation
<b>UWF</b>	Ultra Wide Field
<b>VMD</b>	Variational Mode Decomposition
<b>YOLO</b>	You Only Look Once